Wood Sci Technol (2011) 45:755–765
DOI 10.1007/s00226-010-0394-7

ORIGINAL

Comparison of two optical methods for contactless, full field and highly sensitive in-plane deformation measurements using the example of plywood

Andreas Valla · Johannes Konnerth · Daniel Keunecke · Peter Niemz · Ulrich Müller · Wolfgang Gindl

Received: 17 February 2010 / Published online: 14 December 2010

Abstract In the present paper, the suitability of Electronic Speckle Pattern Interferometry (ESPI) and Digital Image Correlation (DIC) for the measurement of two-dimensional strain distribution on mechanically stressed wood specimens is evaluated. Particular attention is dedicated to the basics of the individual techniques in order to discuss potential advantages and disadvantages. The results of a model experiment with plywood show that the results delivered by both methods are very similar and of high quality. ESPI provides reasonably fast experimental set-up and data acquisition, and fast, straightforward post-processing. Compared to ESPI, DIC is a more versatile method demanding skilled sample preparation, and post-processing may be time consuming.

Introduction

The measurement of displacements and strains (displacement gradients) is an important topic for the mechanical characterization of solid materials. Since wood has a hierarchical and inhomogeneous structure over a wide range of scales,

A. Valla · J. Konnerth · W. Gindl (✉)
Institute of Wood Science and Technology,
Department of Material Sciences and Process Engineering,
BOKU—University of Natural Resources and Applied Life Sciences,
Peter Jordanstrasse 82, 1190 Vienna, Austria
e-mail: wolfgang.gindl@boku.ac.at

D. Keunecke · P. Niemz
Institute for Building Materials, Department of Civil,
Environmental and Geomatic Engineering,
ETH—Swiss Federal Institute of Technology Zurich, Zurich, Switzerland

U. Müller
Competence Centre for Wood Composites and Wood Chemistry, Linz, Austria

measuring methods for macro-, micro- and nanoscales are necessary. Macroscale measurements can be done with strain gauges, mechanical extensometers, video-extensometers, or simply by computation on the basis of machine cross-head displacement. To detect strain inhomogeneities in wood-based materials in micro- or even nanoscale, several optical, contactless, full field techniques are available. Two recent methods are ***E**lectronic **S**peckle **P**attern **I**nterferometry* (ESPI) and ***D**igital **I**mage **C**orrelation* (DIC). Both methods use different principles to measure the displacement on a sample surface. The field of application and the complexity for the measuring setup differs depending on the experimental conditions and assumptions. In a specific case, either both methods can be used, or one outperforms the other. As previous investigations have shown, both techniques are highly suitable for microscale measurements on wood (Zink et al. 1995; Gingerl 1998; Eberhardsteiner 2002; Samarashinghe and Kulasiri 2004; Gindl et al. 2005; Serrano and Enquist 2005; Konnerth et al. 2006).

For the present study, a simple uniaxial tensile experiment was planned with the goal to compare both techniques on a wood composite under real measuring conditions. Therefore, measuring conditions that can be handled by both methods without a problem were chosen. Particular attention was dedicated to a well-founded assessment of relevant parameters such as spatial resolution and displacement accuracy with regard to the two techniques. For a better understanding, a short discussion of the physical principles of both methods is also given.

Basic principles

ESPI

ESPI is a 3D gauging technique based on the principle of the Michelson Interferometer that enables contactless, full field displacement measurements. In the present study, only the in-plane dependency is considered. When a diffuse reflecting surface is illuminated with two coherent, widened laser beams from two different directions, and an optical setup is used to capture the superposition of both reflected light waves, a speckle-interferogram will result (Jones and Wykes 1989). This is called the speckle effect, which produces a constant speckle pattern with a characteristic mean speckle diameter representing the microstructure of the material (see Fig. 1). Due to the speckle effect, a specific small area on the surface is depicted as a corresponding grey value, which results in a position-dependent mapping with high spatial resolution. Deformation on the sample surface causes a new phase difference between the two laser beams and thus a new speckle interferogram. It is possible to describe deformations of the object caused by mechanical loading, as a function of changing interference-phase between the two laser beams. Two different analysis modes are applicable, a real-time and a phase-shift mode. The real-time mode subtracts the speckle pattern of the loaded sample pixel per pixel from the speckle pattern of the initial state, which produces an image with typical fringe pattern, where object points with identical grey values have the same displacement and object points on neighbouring stripes show displacement with the same absolute value in or against the

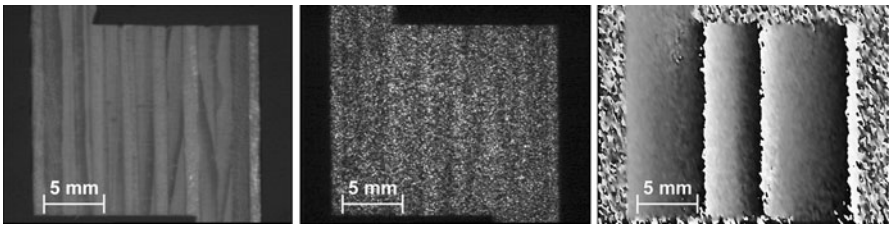

Fig. 1 Images taken during ESPI experiment. *Left*: picture of the sample surface taken with the optical system of the ESPI. *Centre*: speckle-interferogram through sample illumination with a laser beam. *Right*: calculated Modulo 2π Stripeorder-Image

sensitive vector direction. This method is fast and enables real-time measurements, and a first assessment of displacements is possible by analyzing the shape and the frequency of the visible fringes. Detection of high sample deformations and displacements is limited by the number of fringes. In practice, a maximum of 1–10 fringes per load or displacement step leads to convenient results. A series of steps can be summed to measure higher displacements and deformations (Müller et al. 2005).

Unfortunately, this method is incomplete because it does not comprise any information about the direction of displacement, and the fringe pattern does not allow any sub-fringe resolution higher than half an order of interference. This problem can be solved with the phase-shift mode, which uses several measurements under controlled phase shift to create and solve a linear system of equations. Usually, 5 data collections are in progress, resulting in a data collection time of about 0.5 s for one deformation state and direction. Figure 1 shows a so-called Modulo-2π-Stripeorder-Image calculated by using the phase-shift mode. A theoretical accuracy/resolution of about one hundredth of the laser wavelength, i.e., approx. 10 nm, can now be achieved. For further information about the ESPI principles see Gingerl (1998), Rastogi (2001), Eberhardsteiner (2002), Müller et al. (2005).

DIC

The core of DIC is the monitoring of the in-plane displacements on a plane object by tracking deformation of a random pattern in an image. This application enables to identify variations in nearly similar pattern images, which are taken before and after deformation. A complex software detection algorithm is used to cover these small changes in the pattern examined. For a given subset, which is the parameter that defines the size of the investigated area, the correlation algorithm uses an outer loop to identify a given stochastic pattern between two pictures by a classic correlation function. In the next step, an inner loop tries to find an optimization of the correlation function in *sub-pixel* values to find the best displacement with sub-pixel accuracy/resolution of up to one hundredth pixel.

During image acquisition, especially for high deformations, changing of the pattern is probable, e.g., an initially square subset is likely to be deformed. To embrace this during analysis, the deformation transformation is modelled and used

to anticipate the deformed subset. According to this basic principle, certain requirements for the measuring setup have to be fulfilled. Since monocular vision cannot distinguish between isotropic deformation of the object and a change in the distance between the object and the camera, the object has to be *planar*, *parallel* and at *constant distance* throughout the whole time of investigation. A large distance between the object and the camera helps minimize a possible error due to possible out-of-plane displacement of the specimen.

For good correlation results, every pixel of the image should have a unique signature, which is determined by the grey values of its surrounding pixels. Therefore, the natural surface pattern or an artificially applied speckle pattern can be used. The following conditions should be fulfilled: the pattern has to be nonrepetitive, isotropic, high contrast and stochastic. To achieve reliable information, the applied pattern, typically a thin layer of lacquer, has to move with the surface even for large strains, the pattern has to be resistant against impact, changing temperature, moisture and other environmental factors. The size of the subset area depends on the quality of the random pattern and determines the results of the calculations. With the DIC technique, real-time observation is not possible, and the computational processing of the measured data can take up to several hours. However, compared to ESPI, the acquisition of one deformation state only needs one measurement of about 1–100 ms at good ambient light conditions.

Significant parameters

DIC by means of VIC 2D software

Basically, two parameters characterize optical measurements: the spatial resolution of the displacement map and the displacement accuracy. In addition, the magnification factor, which is the length of the field of view (FOV) divided by the number of pixels in the corresponding direction, is of relevance. Finally, the influence of the average speckle size of the generated speckle pattern has to be considered. In the case of DIC, the mean speckle diameter, the spatial resolution and the displacement accuracy are directly influenced by the magnification factor of the image. A first rule of thumb suggests that the mean speckle diameter should be equal to three pixels. Bigger speckles are possible, but they degrade the spatial resolution, whereas smaller speckles degrade the correlation result. The second rule of thumb suggests a subset size that includes at least 3 speckles. Smaller mean speckle diameters require a smaller subset area resulting in a better spatial resolution, but the first rule of thumb has to be considered. The largest speckle limits the subset size. The displacement accuracy is theoretically equal to the magnification multiplied by the sub-pixel accuracy/resolution. According to the inner loop algorithm, a sub-pixel accuracy/resolution of 0.1–0.01 is possible. If speckles of sufficiently small size can be produced, microscopy becomes the only limiting factor of the DIC method.

ESPI

In contrast to DIC, there is no interdependence of significant factors with ESPI. The mean speckle diameter has to be in the range of the physical latitude of the semiconductor detector on the CCD sensor, the speckle size can be changed by means of aperture, and high contrast in the video-image can be taken as a sign for appropriate speckle size. The spatial resolution is equal to the magnification, but a lower limit is given by the mean speckle diameter. The displacement accuracy is determined by the geometry of illumination. It is not affected by the optical setup and can be very flexibly adjusted to fulfil the experimental requirements. The displacement accuracy can be adjusted by a few nanometres up to one micron.

Experiment

Tensile shear specimens were manufactured out of plywood boards (Doka Industrie GmbH, Amstetten, Austria). The geometry of the specimen and the area of interest (AOI) are given in Fig. 2. Notches were sawn with a 3.2-mm-thick circular saw and were cut into the plywood board to a depth of approximately 14.5 mm. The specimens were strained in tension by means of a Zwick/Roell Z100 universal testing machine (Ulm, Germany).

ESPI

For ESPI, the surface was sanded with P200 and P400 sanding paper to obtain a suitable surface. To monitor the sample deformation for the area of investigation (Fig. 2), an ESPI Q300 (Dantec-Ettemeyer, Ulm, Germany) was mounted to the universal testing machine in a way that the ESPI device moved at half cross-head speed. Thus, the same position with regard to the AOI was maintained throughout the experiment. The *Q300* gauge sensor has fixed mirrors for illumination, and they result in three measurement-directions, where 1, 2 coincides with the x-, y-axes of the CCD sensor and 3 that is perpendicular to it. Constant ambient light is necessary during the experiment. The Q300 uses a 1/3″ CCD sensor with a 768 × 567 pixel array. The physical latitude of one array element is 6.5 μm, which is in the range of the possible average pixel size. The aperture was adjusted for best contrast in the speckle-interferogram and fringe image. For more stable conditions (no lateral movement and no vibration of the specimen), a pre-stress of 0.04 N/mm^2 was applied to the specimen. To capture the data for one deformation state, in all three directions, approx. 1.5 s is necessary. Therefore, the tensile experiment had to be interrupted in order to capture measurements. Several load steps with strain-controlled stops of 3 s were necessary. Thirteen load steps with increments of 0.005 N/mm^2 were done, which resulted in a maximum stress of 0.105 N/mm^2. This stress level was well below the failure stress of the specimen of 0.75 N/mm^2. Overall, four measurements under identical conditions were done to decrease noise by means of averaging. The calculation of the displacement maps is done pixel by pixel. For this, and for the calculation of the in-plane strain distributions in axial,

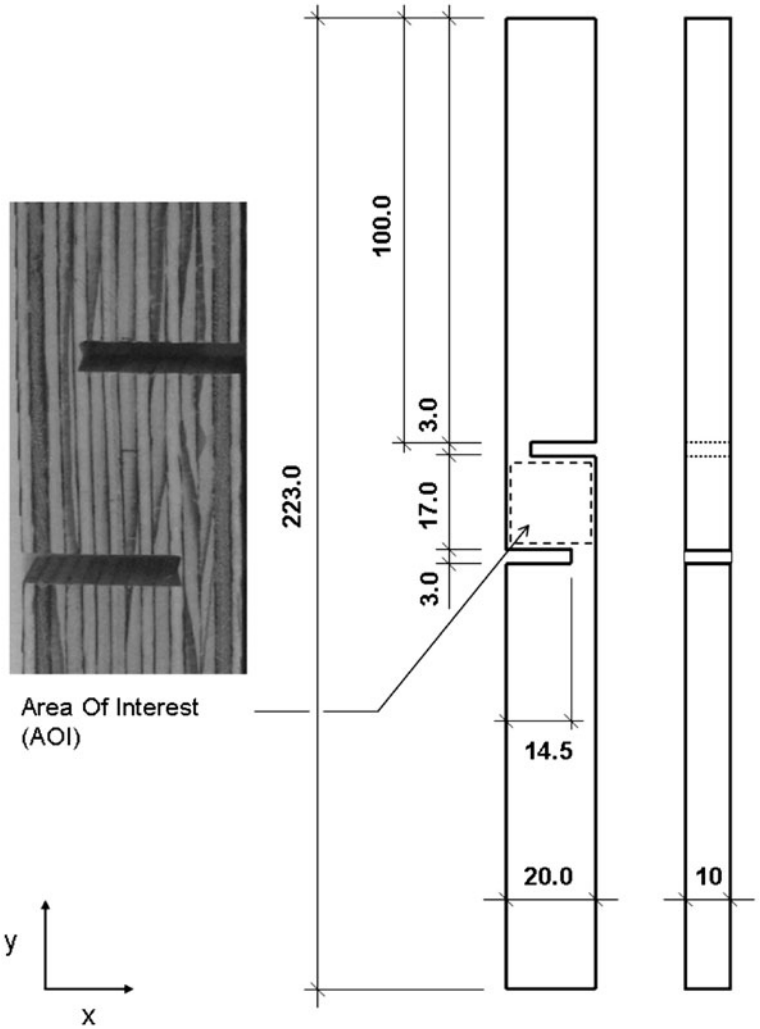

Fig. 2 Dimension of the tensile shear sample given in mm. The *dashed line* marks the area of investigation that was observed during all experiments. The coordinate system x–y coincides with the measurement directions 1–2 of the ESPI Q300 gauge sensor

transversal and shear direction, the post-processing software ISTRA (Dantec-Ettemeyer, Vers. 3.3.12-2001) was used.

DIC

For DIC, an artificial speckle pattern was applied by means of an air-brush system ("EVOLUTION"–Harder & Steenbeck, Oststeinbek, Germany). On a thin primer of white dull acrylic paint, a stochastic distribution of speckles was produced using a nozzle with 0.15 mm diameter and a working pressure of approximately 2.5 bar.

The desired mean speckle diameter for the configuration in the present test setup was in the order of 40 μm. A digital grey value camera (Correlated Solutions Inc., USA) was mounted to the universal testing machine and used for image capture. For constant and bright ambient light, a cold white light source was used. High-contrast and well-focussed images are assured using the snapshot software Vic Snap (Correlated Solutions Inc.) with tools to avoid overexposure and blurred images. The used camera has a 12-bit 2/3″ CCD sensor with a 1,628 × 1,236 pixel array and is able to capture up to 15 frames per second with a minimal exposure time of 31 μs. Same as for ESPI, the load was applied with position controlled cross-head speed of 0.1 mm/min, but no stops for image acquisition were necessary. To guarantee good correlation results, one image per second was taken automatically using the Vic Snap software. The image correlation software Vic-2D (Correlated Solutions Inc., Vers. 4.4.1—2006) was used to calculate the in-plane strain distributions. A reference image in undeformed state and the series of deformed images were selected. For the reference image, the AOI must be chosen, and the subset and step size have to be decided upon. Both have a strong influence on the output of the image correlation algorithm. The step parameter defines which pixel is taken for the calculation, smoothing is done in between. A step size of 3 means that a correlation will be carried out at every third pixel in both horizontal and vertical direction. The subset parameter determines the area which is investigated for the unique fingerprint. A high step value results in faster calculations but can cause glazed images. A large subset results in low spatial resolution, low random noise and high computation time.

Results and discussion

In the following section, the results of an experiment performed with the same specimen using the two different techniques introduced in detail above are presented and discussed. Typical in-plane strain distribution maps for the AOI shown in Fig. 2 are displayed in Fig. 3. A very good discrimination between individual veneer layers of the plywood is given in the shear strain distribution map. It can be seen that layers oriented parallel to the load direction undergo negligible deformation, whereas transversely oriented layers are significantly deformed. In axial direction, the strain distribution is rather uniform, which is plausible, because the individual layers of the plywood cannot move with respect to each other in this direction. By contrast, transverse strain is unevenly distributed, with significant amounts of strain near the notches of the specimen, which is typical for this kind of shear assay (Müller et al. 2005).

In contrast to the calculation of strain maps from ESPI data, which is rather straightforward procedure, digital image correlation requires fine-tuning by adjusting several parameters before an optimum result is obtained. The effect of changes in the two key parameters subset and step on the resulting strain map is evaluated in Fig. 4. An increase in both parameters results in a smoothing of the correlation output. With regard to the step parameter, this smoothing is caused by interpolation over an increasing number of points, whereas reduced spatial

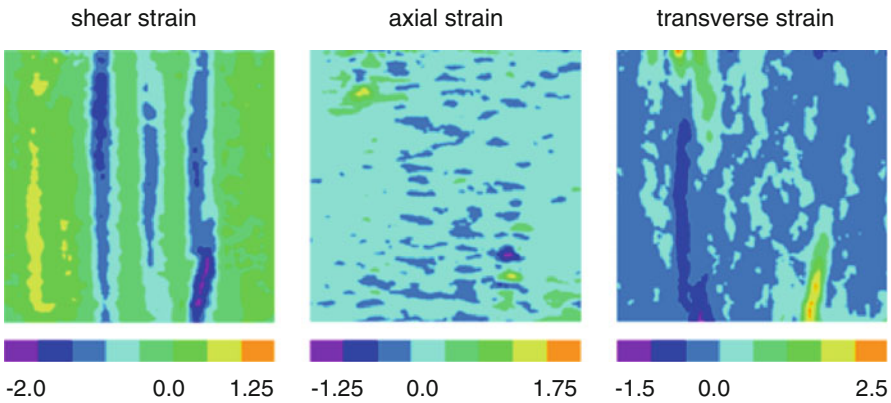

Fig. 3 In-plane strain distribution results for ESPI (μm/mm)

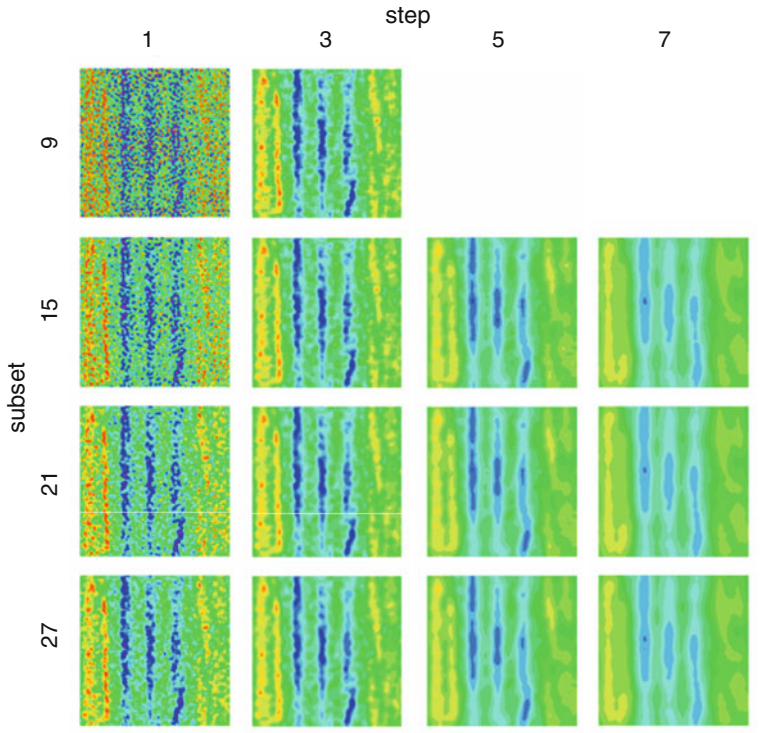

Fig. 4 Shear strain determined with VIC 2D for different pairs of calculation parameters, scaled from −1.5 to 1.5 μm/mm. Horizontal the subset parameter and vertical the step parameter is given

resolution is the cause of a more smooth output with an increasing subset parameter. The step/subset pairs (1/9) and (1/15) show heavily interfered strain maps, and even for (1/21) and (1/27), the results are still far from low-noise. The fact that

correlation succeeded without any problem even for the smallest possible subset value of 9 can be taken as an indicator for the high quality of the artificial speckle pattern applied to the specimen surface. Increasing the step value to 3 leads to much better results independent of the chosen subset value, but the smoothing effect of the subset can still be seen. A further increase in the step parameter yields a smoothed strain map that still shows the main characteristics of strain variability, but the intensity of maximum and minimum values is reduced. To find a compromise between smoothing, high spatial resolution and realistic absolute values, the strain map resulting from the combination (3/15) was selected for further analysis.

In order to obtain strain maps with comparable absolute values, ten ESPI measurements and 30 images for DIC, both up to an end stress level of 0.105 N/mm^2, were considered for the comparison of ESPI and DIC given in Fig. 5. For both methods, a very similar distribution of shear strain was obtained. Overall, high shear strain is found in veneer layers oriented transverse to the loading direction (end-grain view), whereas very low strain was observed for those layers that were parallel to the load direction. Area 1 in Fig. 5 consists of two layers of veneer oriented transversely to the load direction. Correspondingly, high positive shear strain represented by orange colour is seen in both strain maps. These orange zones are associated largely with low-density earlywood zones, whereas high-density latewood shows low shear strain (green colour). The situation is similar in Area 5. The central Areas 2, 3 and 4 represent alternating layers of transversely (high negative shear strain in blue) and axially (low strain in green) oriented veneer. Even fine details such as in Area 6 are represented nicely by both methods. Here, an earlywood band next to a cracked latewood band shows exceptionally high shear strain. Overall, slightly more detail seems to be present in the DIC strain map compared to ESPI. However, on the quantitative level, a very good agreement is obtained between both methods as demonstrated by the excellent correlation of strain values shown in Fig. 6. At the end of this paragraph, the most important features of both techniques discussed in the present study are summarized in Table 1.

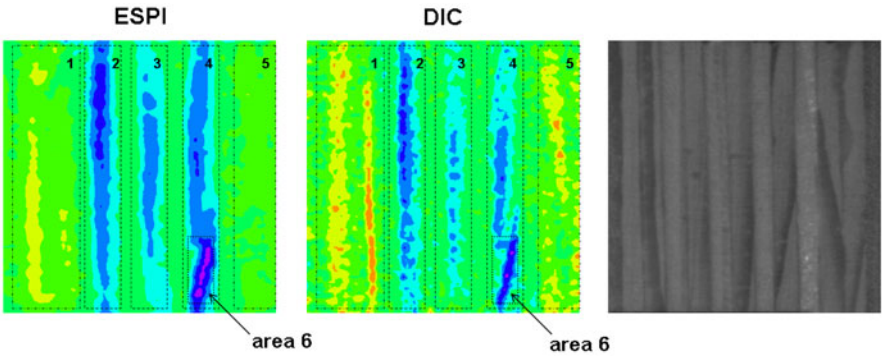

Fig. 5 Comparison of the shear strain shows the numbered areas for the measured mean shear strain

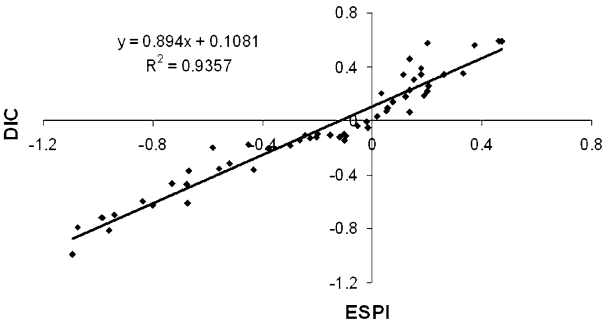

Fig. 6 Correlation of DIC and ESPI shear strain results

Table 1 Comparison of the most important features of ESPI and DIC with respect to the present study

Feature	ESPI	DIC
Experimental set-up	Demands experience	Easy
Data acquisition	Comparably slow, experiment has to be interrupted	Fast, continuous experiment is possible
Data evaluation	Fast	Intermediate to slow (several hours)
Spatial resolution (μm/px)	33	190
Displacement accuracy (nm)	31–78	257
Versatility and flexibility	Good	Outstanding
Cost of investment	Considerable	Moderate

Conclusion

The results of the present study show that both methods, ESPI and DIC, are equally suited for the analysis of strain distribution in a mechanically strained plywood specimen. While both methods deliver comparable results in the present case, the decision on which method to chose depends on the specific application and for experiments where both methods perform equally well, on the cost of investment. Generally, it can be said that with ESPI, success depends primarily on the correct experimental set up, whereas with DIC, surface preparation (artificial speckle pattern) is crucial.

Acknowledgments W. Gindl and A. Valla gratefully acknowledge financial support by the Austrian Science Fund FWF under grant P16837-N07.

References

Dantec—Ettemeyer ISTRA for Windows, Version 3.3.12. Dantec Ettemeyer GmbH, Ulm, Germany, 2001

Eberhardsteiner J (2002) Mechanisches Verhalten von Fichtenholz—Experimentelle Bestimmung der biaxialen Festigkeitseigenschaften. Springer, Vienna—New York

Gindl W, Sretenovic A, Vincenti A, Müller U (2005) Direct measurement of strain distribution along a wood bond line–Part II: Effects of adhesive penetration on strain distribution. Holzforschung 59:307–310

Gingerl M (1998) Realisierung eines optischen Deformationsmesssystems zur experimentellen Untersuchung des orthotropen Materialverhaltens von Holz bei biaxialer Beanspruchung. Doctoral thesis, Vienna University of Technology

Jones R, Wykes C (1989) Holographic and speckle interferometry. Cambridge University Press, Cambridge

Konnerth J, Valla A, Gindl W, Müller U (2006) Measurement of strain distribution in timber finger joints. Wood Sci Technol 40:631–636

Müller U, Sretenovic A, Vincenti A, Gindl W (2005) Direct measurement of strain distribution along a wood bond line. Part 1: Shear strain concentration in a lap joint specimen by means of electronic speckle pattern interferometry. Holzforschung 59:300–306

Rastogi PK (2001) Measurement of static surface displacements, derivatives of displacements, and three-dimensional surface shapes—examples of applications to non-destructive testing. In: Rastogi PK (ed) Digital speckle pattern interferometry and related techniques. Wiley, New York, pp 141–224

Samarashinghe S, Kulasiri D (2004) Stress intensity factor of wood from crack-tip displacement fields obtained from digital image processing. Silva Fenn 38:267–278

Serrano E, Enquist B (2005) Contact-free measurement and non-linear finite element analyses of strain distribution along wood adhesive bonds. Holzforschung 59:641–646

Vic-2D Digital Image Correlation for Windows, Version 4.4.1, build 671 09/26/2005. Correlated Solutions, Inc

Zink AG, Davidson RW, Hanna RB (1995) Strain measurement in wood using a digital image correlation technique. Wood Fiber Sci 27:346–359